

# Measurements of flame propagation velocities and blast wave pressures for methane/oxygen gas mixtures

Dongjoon Kim<sup>\*†</sup>, Shu Usuba<sup>\*</sup>, Yasuhide Watanabe<sup>\*\*</sup>,  
Toshihisa Nario<sup>\*\*</sup>, and Yozo Kakudate<sup>\*</sup>

<sup>\*</sup>National Institute of Advanced Industrial Science and Technology, 1-1-1 Higashi, Tsukuba, Ibaraki 305-8565, Japan

<sup>†</sup>Corresponding address : dj-kim@aist.go.jp

<sup>\*\*</sup>Japan Aerospace Exploration Agency, 2-1-1 Sengen, Tsukuba, Ibaraki 305-8505, Japan

Received : November 17, 2011 Accepted : February 24, 2012

## Abstract

The flame propagation and the blast wave behaviors of methane/oxygen gas mixtures have been investigated. The mixtures were charged into spherical transparent rubber balloons and ignited at its center. The flame propagation behaviors were recorded by a high-speed video camera and the blast wave pressures were measured by several piezoelectric sensors. Although different scale experiments were conducted, the flame propagation behaviors for the same equivalence ratio are similar to each other, and the velocity increased continuously during the flame propagation. The pressure-time histories showed a continuous rise of pressure immediately after the blast wave was formed in air. However, as the blast wave traveled, a discontinuity appeared which resulted in the formation of a shock wave. Eventually, the blast wave lost its discontinuity at long distances. Trinitrotoluene (TNT) equivalents for the mixtures were evaluated by comparing the peak pressures and the impulses with those for TNT. It was found that TNT equivalents near the explosion source are smaller than those at long distances, while they can be considered as constant if evaluated using the impulse at a sufficiently long distance.

**Keywords** : gas explosion, flame propagation velocity, blast wave, TNT equivalent, scaling law

## 1. Introduction

The Japan Aerospace Exploration Agency (JAXA) has been developing a propulsion system using liquid oxygen (LOX) and liquefied natural gas (LNG) that has methane as the principal ingredient, and safety evaluations of the rocket has been conducted with this propulsion system. One of the accident scenarios is that the rocket falls back down for some reason after setting in a launch pad. If LOX and LNG leak from the fuel tanks of the rocket and spread on the ground surface, the vapor cloud composed of methane and oxygen is formed by the evaporation of LOX and LNG. It is noteworthy that methane and oxygen can coexist in the liquid phase, in contrast to hydrogen and oxygen. The methane/oxygen gas mixture has very low ignition energy<sup>1)</sup> and thus it can be easily ignited. Formation of the vapor cloud reveals a high potential hazard with the risk of an accidental explosion that could cause serious damage over the far distance.

In case of the detonation of explosives, the evaluation methodology for the trinitrotoluene (TNT) equivalent is established based on the blast pressure characteristics and is applicable over a wide range of explosive mass using the scaling law of cubic root. However, although there have been many studies on the blast wave generated from the deflagration of various gases<sup>2)-4)</sup>, Generation and propagation characteristics of the blast wave and the evaluation of the TNT equivalent are still not sufficiently understood.

Considering this, explosion experiments using methane/oxygen gas mixtures of the order of 10 g to 1 kg in mass were conducted, and the propagation behaviors of the flame and the blast wave were investigated in detail and the evaluation of TNT equivalent was attempted.

## 2. Experimental

The experimental setup to investigate flame

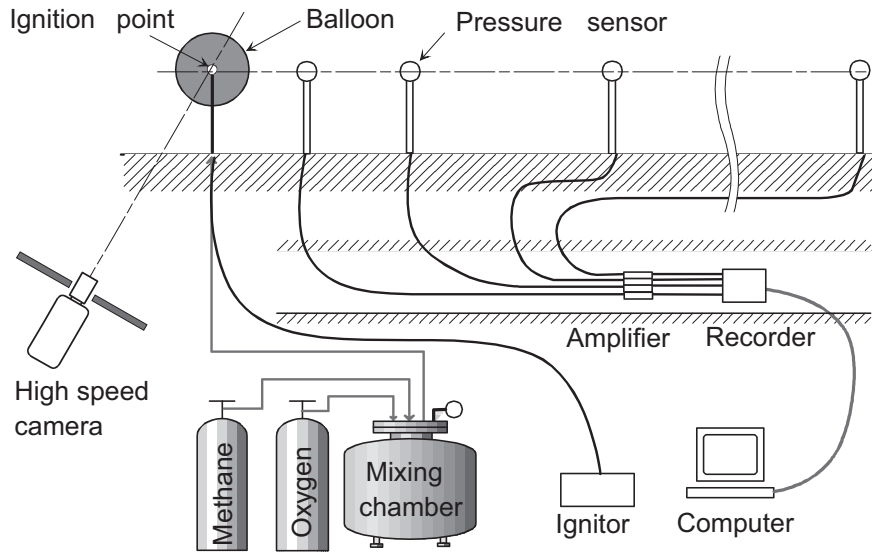


**Figure 1** Experimental setup to investigate flame propagation velocities and blast wave pressures.

**Table 1** Experimental conditions

Equivalent ratio, $\phi$	Diameters* [m]	Volume [m <sup>3</sup> ]	Gas mass [g]	Inner pressure [kPa]	Ambient pressure [kPa]	Ambient temperature [°C]
1.00	0.23	0.0076	9.1	102.2	99.1	8
1.00	0.45	0.0329	39.3	100.6	98.8	10
1.00	0.60	0.102	122.2	101.4	98.6	15
1.00	0.90	0.260	309.8	100.1	98.7	9
0.60	0.90	0.245	315.2	100.4	99.1	10

\*Nominal balloon diameter

propagation velocities and blast wave pressures is shown in Figure 1. Methane and oxygen are mixed in a mixing chamber with controlling their partial pressures to obtain a required methane concentration. The mixtures are then charged into spherical transparent rubber balloons. The mass of charged gas is calculated from the pressure drop of the mixing chamber, the volume of which is measured in advance. The experimental conditions are summarized in Table 1. The experiments were conducted mainly for stoichiometric mixtures (equivalent ratio,  $\phi$ , of 1.00)

The mixtures are ignited at the center of the balloons by a fused Nichrome wire (0.1 mm diameter and 6 mm long). The firing current flowing through the Nichrome wire is a discharge current from an electrolytic capacitor and formed into a single square wave by an electronic load.

Blast wave pressures are measured by several piezoelectric sensors (PCB, 102A07, 106B50) placed at 1.00–75.00 m from the ignition point in a straight line. Signals are conditioned with pre-amplifiers and recorded on a waveform digitizer at a sampling rate of 1 MS/s. Ignition and flame propagation behaviors in the balloon are observed with a high-speed video camera (Vision Research, Phantom v640) at 10,000 fps.

### 3. Experimental results and discussions

#### 3.1 Flame propagation

As an example, the framing images obtained with a high

speed video camera while a flame propagates through the stoichiometric gas mixture of 309.8 g are shown in Figure 2. The initial of time is when the gas was ignited, and every 4th frame (0.4 ms interval) is shown in the figure. A flame emits visible light, blue, so the position of the flame front is easily confirmed.

Radial positions of the flame front ( $R_f$ ) are plotted as a function of time in Figure 3. The symbols of X+, X-, Y+ and Y- represent the directions given in Figure 2. Because the flame propagation behaviors of the four directions agree very well, it is considered that the flame propagates with good spherical symmetry and the effect of gravity is negligibly small under the experimental conditions.

Furthermore, acceleration of the flame is observed. In fact  $R_f$  can be expressed well as a quadratic polynomial of time, as shown with a solid line in Figure 3. In general the flame acceleration is attributed to the generation of turbulent flow in the flame, which results in an increase of the energy release rate.<sup>5)–7)</sup> Gostintsev *et al.*<sup>5)</sup>, however, reported that there exist self-similar region of propagation of the front of a completely developed turbulent flame, and in this region

$$R_f = R_1 + At^{3/2} \quad (1)$$

is derived, where  $t$  is the duration from the ignition, and  $R_1$  and  $A$  are empirical constants. The fitted result is also shown as a broken line in Figure 3. There is no significant

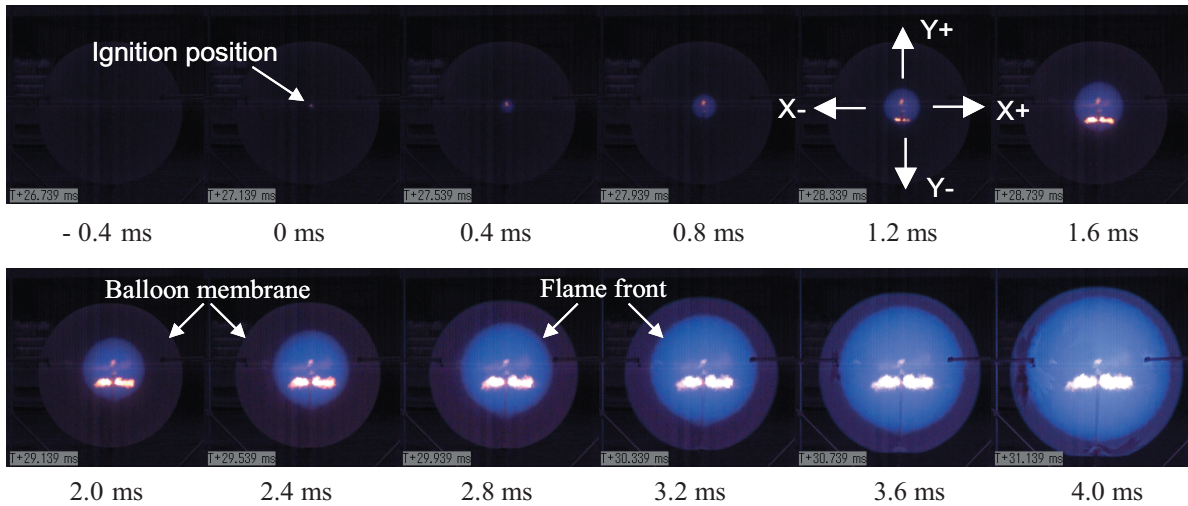


Figure 2 Framing images obtained with a high-speed video camera while flame propagates through the stoichiometric mixture of 309.8 g.

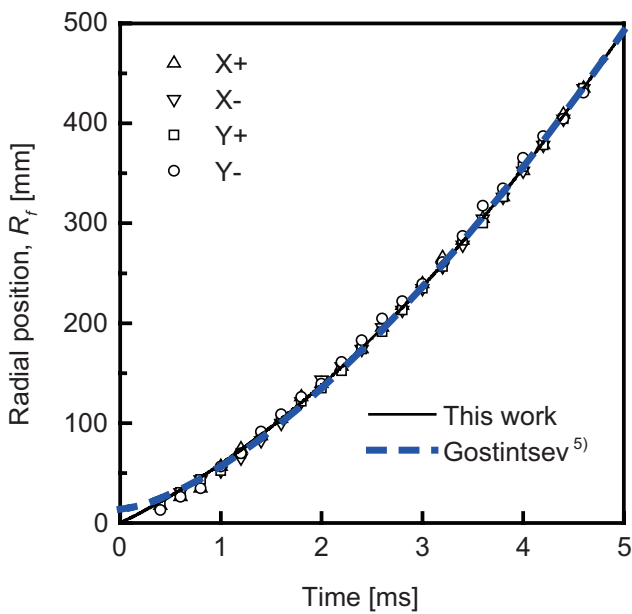


Figure 3 Flame propagation in four directions for the stoichiometric mixture of 309.8 g.

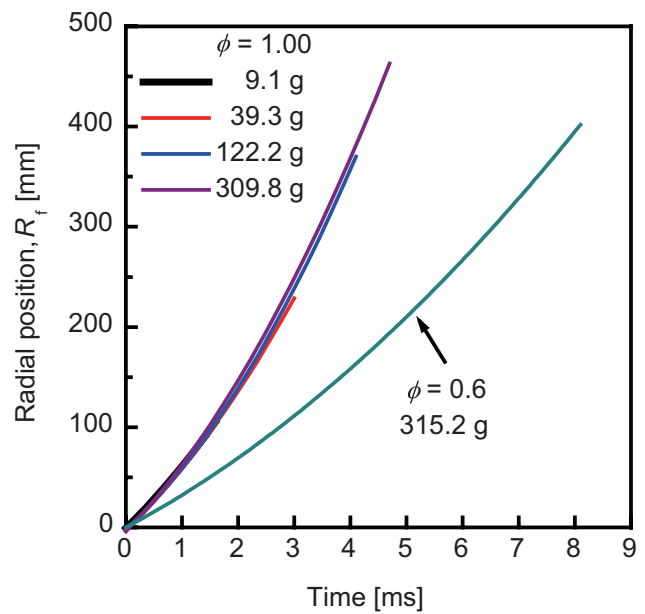


Figure 4 Curve fitting results for radial position of flame by a quadratic polynomial.

difference between the results, which implies that the scale range in the present study is too narrow to judge the validity of the empirical expressions.

Curves fitted with quadratic polynomials for different masses of the stoichiometric gas mixtures as well as a gas mixture with  $\phi = 0.6$  are shown together in Figure 4. The flame propagating through the stoichiometric mixtures after ignition is almost the same, even if the masses of gas mixture, that is, diameters of balloons, are different. And this indicates that the existence of the balloon membrane does not significantly affect the flame propagation.

Flame propagation velocities that are obtained by differentiating the quadratic polynomials to fit the flame position with respect to time are shown as functions of time in Figure 5. The initial flame propagation velocity ( $V_{f0}$ ) is approximately 55 m/s. It is possible to estimate  $V_{f0}$  with another method;  $V_{f0}$  is a product of the burning velocity ( $S_L$ ) and expansion ratio ( $\beta$ ), that is, the density ratio of the burnt gas to the unburnt gas.<sup>8),9)</sup> Plausible values of  $S_L = 4.4$  m/s and  $\beta = 12.5^{10-12)}$  lead to  $V_{f0} = 55$  m/s

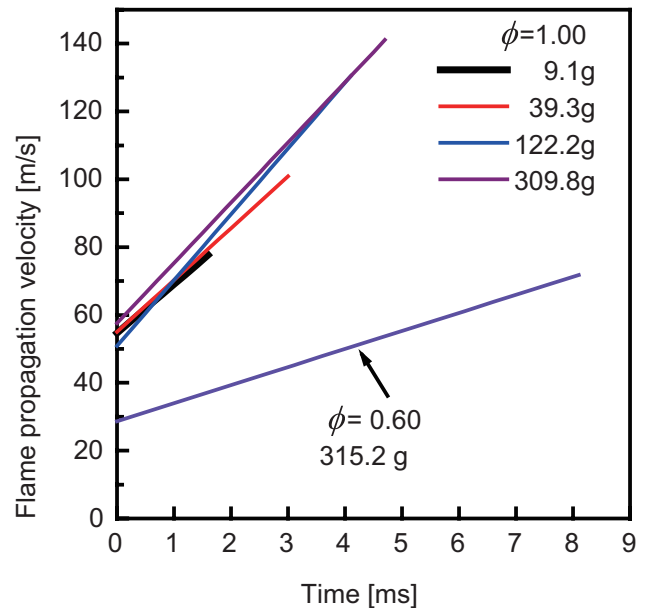


Figure 5 Flame propagation velocities

that agrees well with the present experimental result.

For the largest diameter of the balloon, mass of 309.8g, the final flame propagation velocity reaches about 140m/s. Simple extrapolation of the flame propagation velocity for a larger balloon suggests that it is plausible that the flame propagation velocity probably overtakes the sound velocity. Therefore, it is expected that deflagration to detonation transition might be observed in a considerably large-scale experiment.

### 3.2 Blast wave

Figure 6 shows the pressure–time histories of the blast wave for the stoichiometric mixture of 309.8g at the distance of each sensor. These have different features from the pressure–time history produced by the detonation of an explosive. The pressure–time history at 1.01 m shows a continuous rise of pressure immediately after the blast wave was formed in air, because the flame propagation velocity is smaller than the sound velocity of the mixture. However, as the blast wave travels, a discontinuity appears at 2.03m and grows, resulting in the formation of a typical shock wave at 10.06m. At long distances greater than 40.02m the blast wave loses its discontinuity gradually. The pressure–time histories for the mass of 9.1g (Figure 7) obviously shows that the discontinuity disappears and is replaced by the sound wave.<sup>13</sup> In the case of  $\phi = 0.60$  no discontinuity was observed, because the flame propagation velocity, in other word, the expansion velocity of the burnt gas, is not so large and the duration of the expansion is not sufficiently long enough to produce a shock wave<sup>14</sup>.

Logarithmic plots of peak overpressure and impulse with respect to scaled distance are shown in Figures 8 and 9, respectively. The impulse and the distance were scaled by the mass of the gas mixture. In each figure, the TNT data summarized by Baker *et al.*<sup>13</sup>, is also shown as a solid

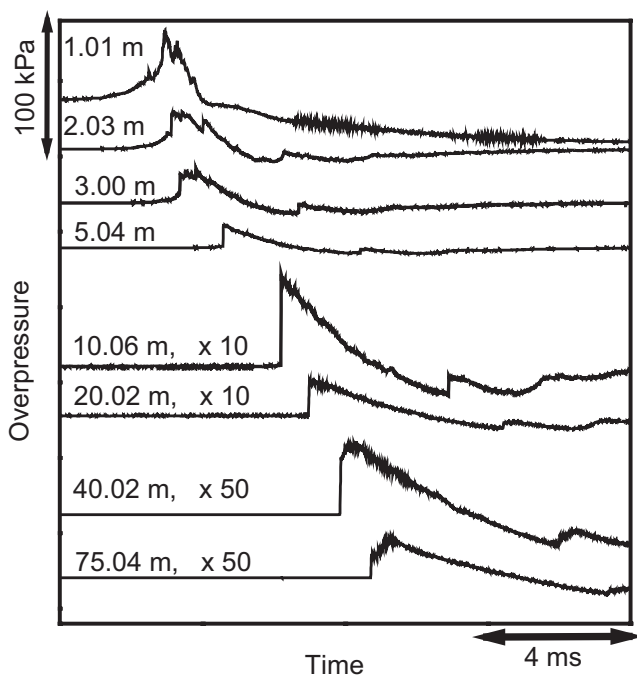


Figure 6 Pressure–time histories of blast wave for stoichiometric mixture of 309.8 g.

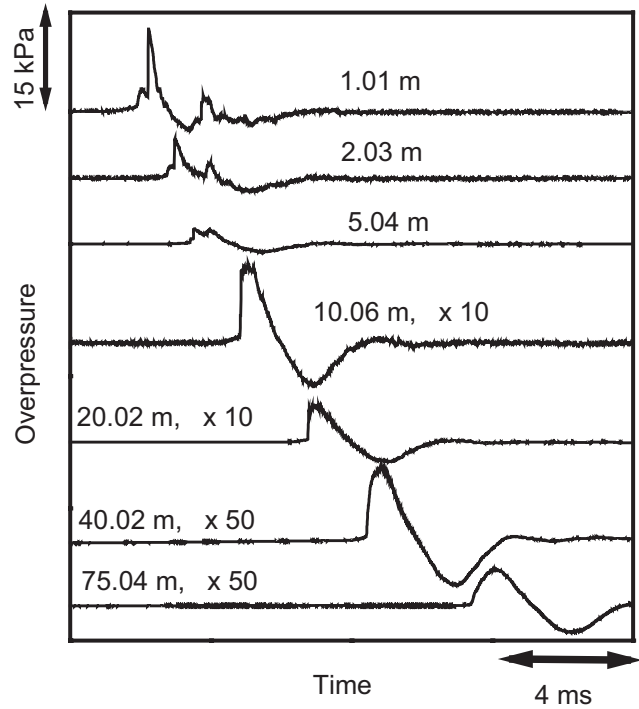


Figure 7 Pressure–time histories of blast wave for stoichiometric mixture of 9.1 g.

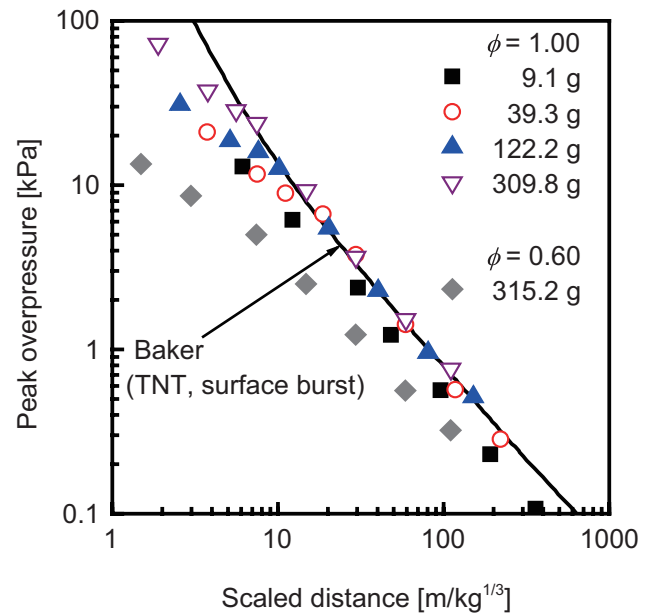


Figure 8 Peak overpressure with respect to the scaled distance.

line. Because Baker's data are obtained for explosions in free air, they are converted to the data on the ground surface by doubling the apparent mass, on the assumption that the ground acts as a perfectly smooth rigid plane against the shock wave.

In the case that the scaled distance is smaller than about 10, the peak overpressure (Figure 8) for the gas mixture with  $\phi = 1.00$  is smaller than that for TNT, and seems to have a different slope from that for TNT in the logarithmic plot. However, in the region of the scaled distance about 10–100, both slopes have a tendency to agree with each other. When the scaled distance is larger than about 100, the slopes for the gas mixture

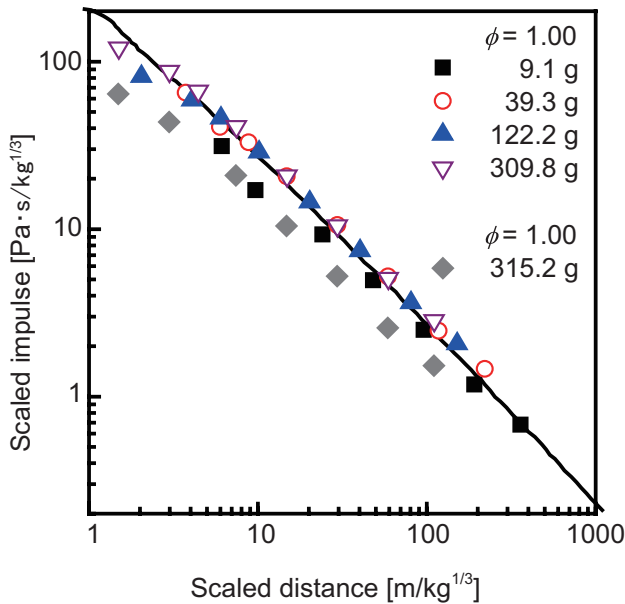


Figure 9 Impulse with respect to the scaled distance.

asymptotically approach  $-1$ , which indicates the blast waves have characteristics of the sound wave. These behaviors are in accordance with the pressure-time histories of the blast wave shown in Figures 6 and 7. When  $\phi = 0.60$ , the second region mentioned above seems to banish because no shock wave is produced. Similar tendency is seen for the impulse, as shown in Figure 9.

TNT equivalents of the stoichiometric gas mixture were evaluated at each distance by comparison of the overpressures and the impulses for TNT. Ratios of the TNT equivalent to the mass of the gas are plotted as a function of the distance in Figure 10. It is found that TNT equivalents near the explosion source are smaller than those for long distances, while they can be considered as constant if evaluated by using the impulse at sufficiently a long distance. In Figure 10 the values evaluated by using the peak overpressure as TNT equivalents are scattered in the region of 3–10m. This might come from the followings. In this region a shock wave is growing up and complex phenomena such as the interference of sound waves and/or shock waves similar to the formation of Mach stem should occur.

#### 4. Conclusions

The flame propagation behaviors and the blast wave pressures of methane/oxygen gas mixtures have been investigated. Although experiments of different scales were conducted, the flame propagation behaviors for the stoichiometric mixture are similar to each other, and the velocity increases continuously during the flame propagation. The pressure-time histories showed a continuous rise of pressure immediately after blast wave was formed in air. However, as the blast wave traveled, a discontinuity appeared resulting in a formation of a shock wave. The TNT equivalents show that the values near the explosion source are smaller than those at far distances. Eventually, at long distances the blast wave lost its discontinuity. If the TNT equivalents are evaluated by

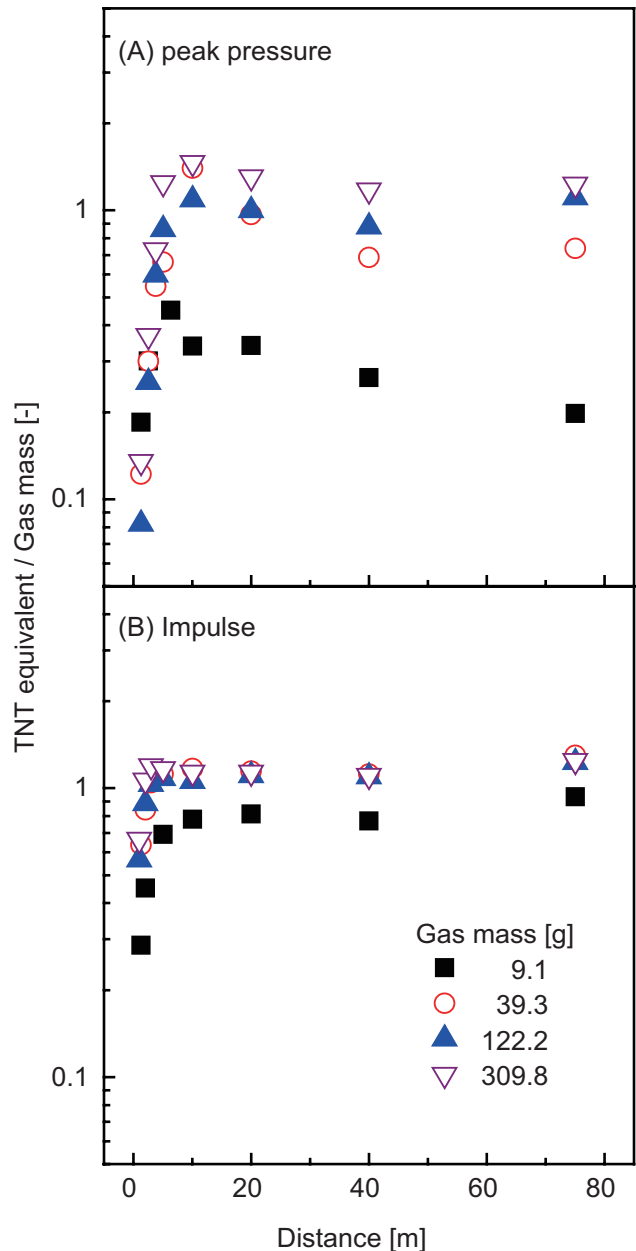


Figure 10 TNT equivalent for the stoichiometric mixture calculated with peak overpressure (A) and impulse (B).

using the impulse at long distances, they can be considered as constant, and can be estimated by the scaling law of cubic root.

#### References

- 1) B. Leqis, G. von Elbe, "Combustion, Flames and Explosions of Gases (Third Edition)", p. 343, Academic Press, London (1987).
- 2) S. M. Kogarko, V. V. Audshkin, and A. G. Lyamin, Combustion, Explosion, and Shock waves, 1, 15 (1965).
- 3) J. C. Leyer, D. Desbordes, J. P. Saint-Cloud, and A. Lannoy, Journal of Hazardous Materials, 34, 123 (1993).
- 4) K. Wakabayashi, Y. Nakayama, T. Mogi, D. KIM, T. Abe, K. Ishikawa, E. Kuroda, T. Matsumura, S. Horiguchi, M. Oya, and S. Fujiwara, Sci. Tech. Energetic Materials, 68, 25 (2007).
- 5) Y. A. Gostintsev, A. G. Istratov, and Y. V. Shulenin, Combustion, Explosion and Shock waves, 24, 563 (1988).

- 6) A. Gaydon and H. Wolfhard, "Flames: Their structure, Radiation and Temperature", p.4, Chapman and Hall (1979).
- 7) K. Mukaiyama, K. Kuwana, Journal of Loss Prevention in the Process Industries, (In press).
- 8) G. C. Andrews and D. Bradley, Combustion and Flame, 18, 133 (1972).
- 9) O. C. Kwon and G. M. Faeth, Combustion and Flame, 124, 590 (2000).
- 10) B. Lewis and G. Elbe, "Combustion, Flames and Explosions of Gases, 3rd ed.", pp. 348–351, Academic Press (1987).
- 11) W. A. Strauss and R. Edse, Seventh symposium on Combustion, pp. 337–385, The Combustion Institute (1958).
- 12) S. Y. Kazantsev, Il G. Kononov, I. A. Kossyi, N. M. Tarasova, and K. N. Firsov, Plasma Physics Reports, 35, 252 (2009).
- 13) W. E. Baker et al. "Explosion Hazards and Evaluation", p. 121 Elsevier Scientific Publishing company, Amsterdam (1983); *ibid.* p.207.
- 14) G. T. Taylor, Proceedings of the Royal Society, A186, 273 (1946).